

One-Electron State of a Partially Ionized High-Z Ion

Yoichiro FURUTANI*, Hiroo TOTSUJI*,
Kunitaka KOMAKI* and Masahiro TANABE *

(Received March 16, 1988)

Synopsis

An effective potential of an isolated partially ionized high-Z ion, calculated within the framework of the statistical models of atoms, is injected into the one-electron Schrödinger equation, in view of evaluating the electron density and comparing it with the results of statistical models. Starting from this initial value, a self-consistent electron density is obtained on the basis of the density functional theory, where quantum natures of electrons are fully taken into account.

§1. Introduction

In laser-driven fusion plasma experiments, we always encounter partially ionized heavy impurity ions emitted from the pellet and the pusher. Their effects on such transport phenomena as the electric and thermal conduction and the radiative transfer are not yet well understood and we are urged to clarify them from the viewpoint of both the elementary atomic processes and the MHD transport.

In order to study an internal state of these partially stripped high-Z ions, we have worked out a model of an isolated ion within the framework of the statistical model of atoms in Ref.1, which will be quoted as I in this paper. (The term "ion" will be used also for neutral atoms, since they can be viewed as ions with no net charges.)

Our next task is to check the consistency of the statistical model, either Thomas-Fermi-Dirac (TFD) or Thomas-Fermi-Dirac-

* Department of Electrical and Electronic Engineering

Weizsäcker (TFDW), with the density functional theory (DFT) where electrons are treated quantum mechanically. For this purpose, we inject the effective potential obtained from such a model into the one-electron Schrödinger equation, calculate the electron density anew and compare it with a result of the statistical model. If there were a satisfactory agreement between them, we would claim the validity of the statistical model, i.e., replacement of the quantum mechanical DFT for many-electron problem by simpler models as far as the electron density distribution and Coulombic potential field around ions are concerned. We also try to obtain the self consistent electron density within the DFT starting from the result of models as an initial value.

To corroborate our isolated ion model characterized by an abrupt jump of the electron density at the surface of the ion, we also examine in some detail the asymptotic behavior of the electron density analytically and conclude that, at least for finite temperature models, strictly isolated ions cannot be described by the statistical treatment.

In §2, redundant as it is, we give a brief survey of the statistical model and fix the notations in this paper. In §3, numerical solution of the Schrödinger equation is presented. To obtain a self-consistent distribution of electrons, we have adopted an iterative method borrowing the result of the statistical model as an initial input. In §4, an analysis of the asymptotic behavior of the electron density is given, to justify a posteriori its divergence frequently observed in numerical analysis. Finally, several comments and concluding remarks are summarized in §5.

§2. Survey of the Statistical Models

According to the DFT, on which the statistical models, TFD and TFDW, are based, the electron density $n(r)$ in the TFDW model is determined by the differential equation^{1),2)}

$$\frac{\partial F_K}{\partial n} - \frac{\partial}{\partial n} \left(\frac{\hbar}{n} \right) (\nabla n)^2 - 2\hbar \frac{\nabla^2 n}{n} + \frac{\partial F_{XC}}{\partial n} = \mu + U, \quad (1)$$

where $F[n(r)]$ is the energy density and $U(r)$ defined by

$$U(r) = \frac{Z}{r} - \int dr' \frac{n(r')}{|r-r'|} \quad (2)$$

is the Hartree potential. The subscripts K, X, and C denote kinetic, exchange, and correlation, respectively. The functional $h[n(r)]$ characterizes the effect of the density gradient and is given, as in I, by

$$h(n) = -\frac{1}{12} y \frac{\partial}{\partial \alpha} \left(\frac{1}{I_{-1/2}(\alpha)} \right), \quad y = \frac{\pi^2}{2^{1/2}} n \beta^{3/2}, \quad (3)$$

where α is related to y through the expression

$$y = I_{1/2}(\alpha). \quad (4)$$

We follow the notations in I and use the atomic units unless otherwise specified.

Precision of the whole theory relies upon the appropriate choice of the functional F_{XC} as well as the functional h which partly expresses the nonlocal effect. We here adopt again the local approximation and borrow a fitting formula devised by Tanaka, Mitake, and Ichimaru³⁾ (TMI) on the basis of the Singwi-Tosi-Land-Sjölander (STLS) scheme.⁴⁾

It should be emphasized that eq.(1) has been derived, using the boundary condition $n'(R)=0$. Eq.(1) is then coupled with the Poisson equation

$$\phi^{(2)}(r) = 4\pi r n(r)/Z \quad (5)$$

to determine $\phi(r)$ and $n(r)$, where $\phi(r)$ is defined as

$$(Z/r)\phi(r) = \mu + U(r) + K_X^2/4K_T \quad (6)$$

with $K_T = (3\pi^2)^{2/3}/2$ and $K_X = -(3/\pi)^{1/3}$. Neglect of the gradient

correction terms in eq.(1) yields the TFD equation

$$\frac{\partial F_K}{\partial n} + \frac{\partial F_X}{\partial n} = \frac{Z}{r} \phi(r) - \frac{K_X^2}{4K_T}. \quad (7)$$

Eqs.(1) and (7) hold at any temperature. It is therefore useful to give explicit expressions for $\partial F_X/\partial n$ and $\partial F_K/\partial n$:

$$\frac{\partial F_K}{\partial n} = \frac{\alpha}{\beta} \quad \text{and} \quad \frac{\partial F_X}{\partial n} = -\frac{1}{2\pi^3\beta^2} \left[I_{-1/2}(\alpha) \right]^2 = -\frac{\pi\beta}{(d\alpha/dn)^2}. \quad (8)$$

Evaluation of $\partial F_C/\partial n$ is much more involved, since TMI's expression is a sort of Padé approximant which contains the plasma parameter $\Gamma [= \beta(Ze)^2(4\pi n/3)^{1/3}]$ and the degeneracy parameter T/T_F , with T_F the Fermi temperature. Instead of using an analytic expression, we resort to the numerical differentiation for this term.

§3. Self-Consistent Electron Density in Density Functional Theory

A. Solution of one-electron Schrödinger equation

Once the Hartree potential $U(r)$ and the exchange-correlation potential $\partial F_{XC}/\partial n$ are obtained from the statistical model, we inject them into the one-electron Schrödinger equation⁵⁾

$$\left(-\frac{1}{2} \nabla^2 + V(r) \right) \psi(r) = E \psi(r) \quad (9)$$

to calculate the wave function. Since the one-body potential

$$V(r) = U(r) + \frac{\partial F_{XC}}{\partial n} \quad (10)$$

is spherically symmetric, we expand $\psi(r)$ by the spherical harmonics $Y_{\ell m}(\theta, \phi)$ as

$$\psi(r) = \sum_{\ell, m} R_{\ell}(r) Y_{\ell m}(\theta, \phi), \quad (11)$$

where ℓ and m are the azimuthal and magnetic quantum numbers, respectively. Writing the radial part as $R_{n\ell}(r) = \chi_{n\ell}(r)/r$ and normalizing the distance and the energy as $\xi = Zr$ and $\epsilon = E/Z^2$, we obtain

$$\chi_{\ell}^{(2)}(\xi) + \left[2\{\epsilon - v(\xi)\} - \frac{\ell(\ell+1)}{\xi^2} \right] \chi_{\ell}(\xi) = 0, \quad (12)$$

where $v(\xi) = V(r)/Z^2$. We solve this equation by transforming it into an eigenvalue problem with appropriate boundary conditions by finite difference method.

The electron density $n(\xi)$ is related to the solutions of the one-electron Schrödinger equation as⁶⁾

$$n(\xi) = \sum_{n,\ell} 2(2\ell+1) (R_{n\ell}^b(\xi))^2 f(E_{n\ell}) + \frac{2Z^3}{\pi^2} \int_0^{\infty} d\epsilon f(\epsilon) \sum_{\ell} (2\ell+1) (R_{n\ell}^s(\xi))^2, \quad (13)$$

where the first term on the right-hand side refers to bound electrons, while the second to the free electrons. The function $f(\epsilon)$ is the Fermi distribution function, which reduces to 1 for $\epsilon \leq \tilde{\mu} = \mu/Z^2$.

The one-body potential obtained from the statistical TFDW model was used in the Schrödinger equation as an input to the subsequent iteration. The Hartree potential $U(r)$ inside the ion sphere is smoothly connected to the Coulomb potential z/r at the ion sphere.

An initial chemical potential μ was inferred from the highest energy eigenvalue of levels occupied by electrons, the number of which being specified by a given degree of ionization z/Z . Iteration continues until each energy level converges within a prescribed error or until the relative change of energy eigenvalues per one iteration becomes smaller than 10^{-6} .

One important comment is needed at this point on whether or not we may preclude scattering states. If we insist on the idea that all electrons should be enclosed within the ion sphere, situation in which a potential of an infinite height is present on the spherical interface, it suffices to count only a number of bound electrons for a given value of z/Z . In our isolated ion model, however, this is not the case, since the effective potential prevailing in a sphere is connected smoothly with the Coulomb potential z/r outside the sphere. We should thus address ourselves to both the bound and scattering

states, when solving eq.(12).

B. Numerical results at $T=0$

In the present numerical analysis, we have chosen $Z=20$ (calcium) as in I with $z/Z=0.1, 0.3$ and 0.6 . Several examples of the final values of energy eigenvalues and μ , the potential $U(\xi)$, and the electron density $n(\xi)$ are shown in Table 1 and Figs.1 to 3 in comparison with those obtained from the TFDW model. The solid line represents the result of the TFDW model, and the dotted and dashed lines refer, respectively, to the initial and final (or converged) values of iteration. In figures labelled (a), values of normalized potential $rU(r)/Z$ are shown and we observe a fairly satisfactory agreement between the solid and dashed lines, which indicates the validity of the TFDW model. In (b) of each figure, the radial density profile $n(r)$ is illustrated. Though the curves are plotted in semi-logarithmic scale, a discrepancy between results of the TFDW model and iterative procedure is minute, except in the intermediate region where the density is already low. Figures (c) and (d) depict $n(r)$ and $4\pi r^2 n(r)/Z^{4/3}$ near the origin in an enlarged scale. The shell structure in (d), indicative of the electron number profile in the ion sphere, is smeared out in the statistical model. In (e), we show the integrated number of electrons as a function of radius. We illustrate in Figs.2 and 3 our results for $z/Z=0.3$ and 0.6 , respectively, in order to emphasize the same trend for each quantity of interest. Numerical analysis for finite temperatures is now in progress.

Table 1. Energy levels and chemical potential for TFDW potential and those for the self-consistent DFT potential.

| n ℓ | $z/Z=0.1$ | | $z/Z=0.3$ | | $z/Z=0.6$ | |
|----------|-----------|----------|-----------|----------|-----------|----------|
| | TFDW | DFT | TFDW | DFT | TFDW | DFT |
| 1 s | -144.255 | -144.295 | -147.611 | -147.648 | -158.217 | -158.244 |
| 2 s | -15.005 | -29.710 | -18.262 | -31.693 | -27.564 | -36.902 |
| 2 p | -12.285 | -24.856 | -15.568 | -26.982 | -25.086 | -32.807 |
| 3 s | -1.936 | -3.966 | -4.546 | -6.739 | | |
| 3 p | -1.295 | -2.895 | -3.823 | -5.678 | | |
| μ | -0.894 | -2.895 | -4.452 | -5.678 | -17.913 | -32.807 |

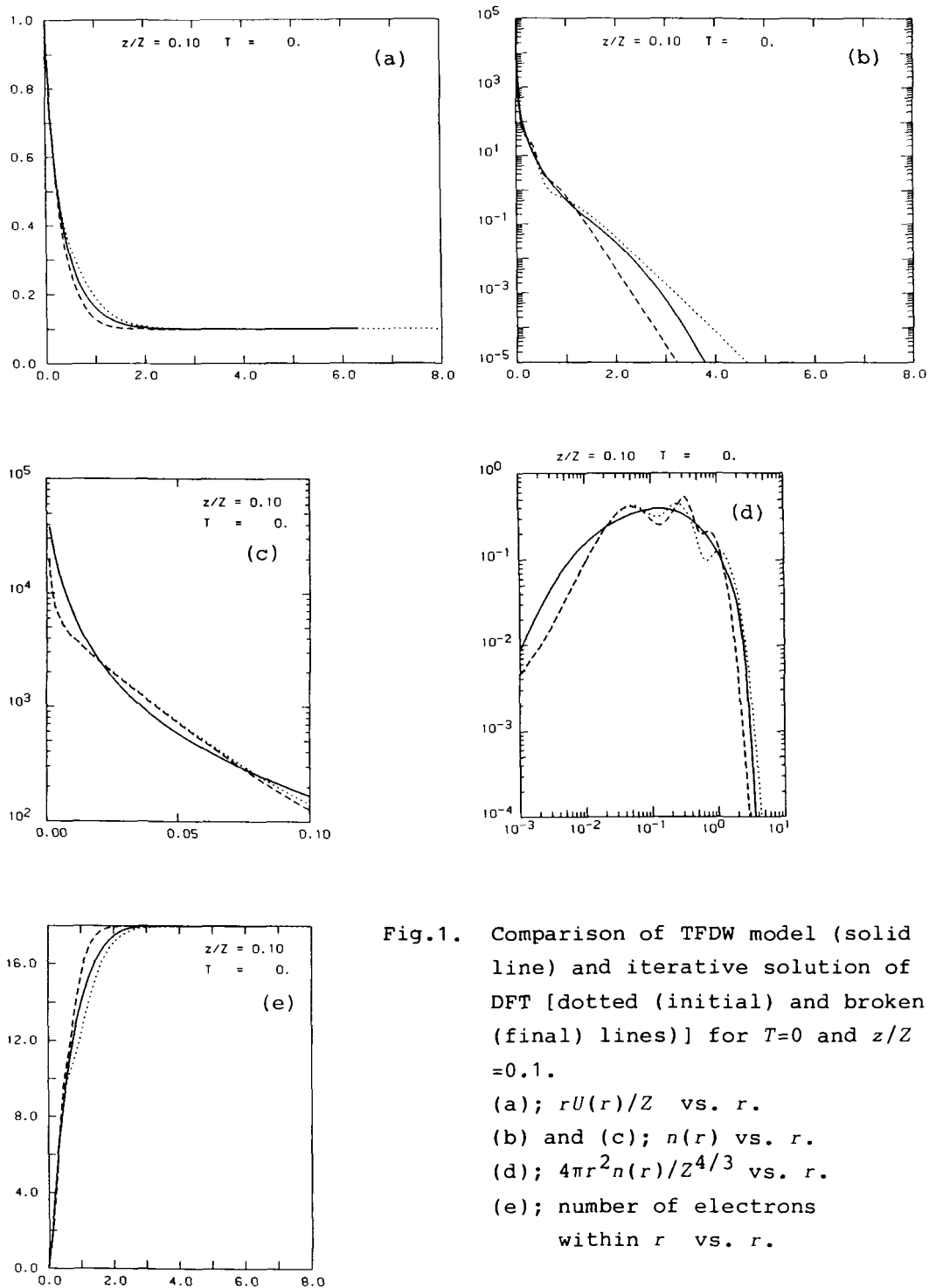


Fig.1. Comparison of TFDW model (solid line) and iterative solution of DFT [dotted (initial) and broken (final) lines] for $T=0$ and $z/Z=0.1$.
 (a); $rU(r)/Z$ vs. r .
 (b) and (c); $n(r)$ vs. r .
 (d); $4\pi r^2 n(r)/Z^{4/3}$ vs. r .
 (e); number of electrons within r vs. r .

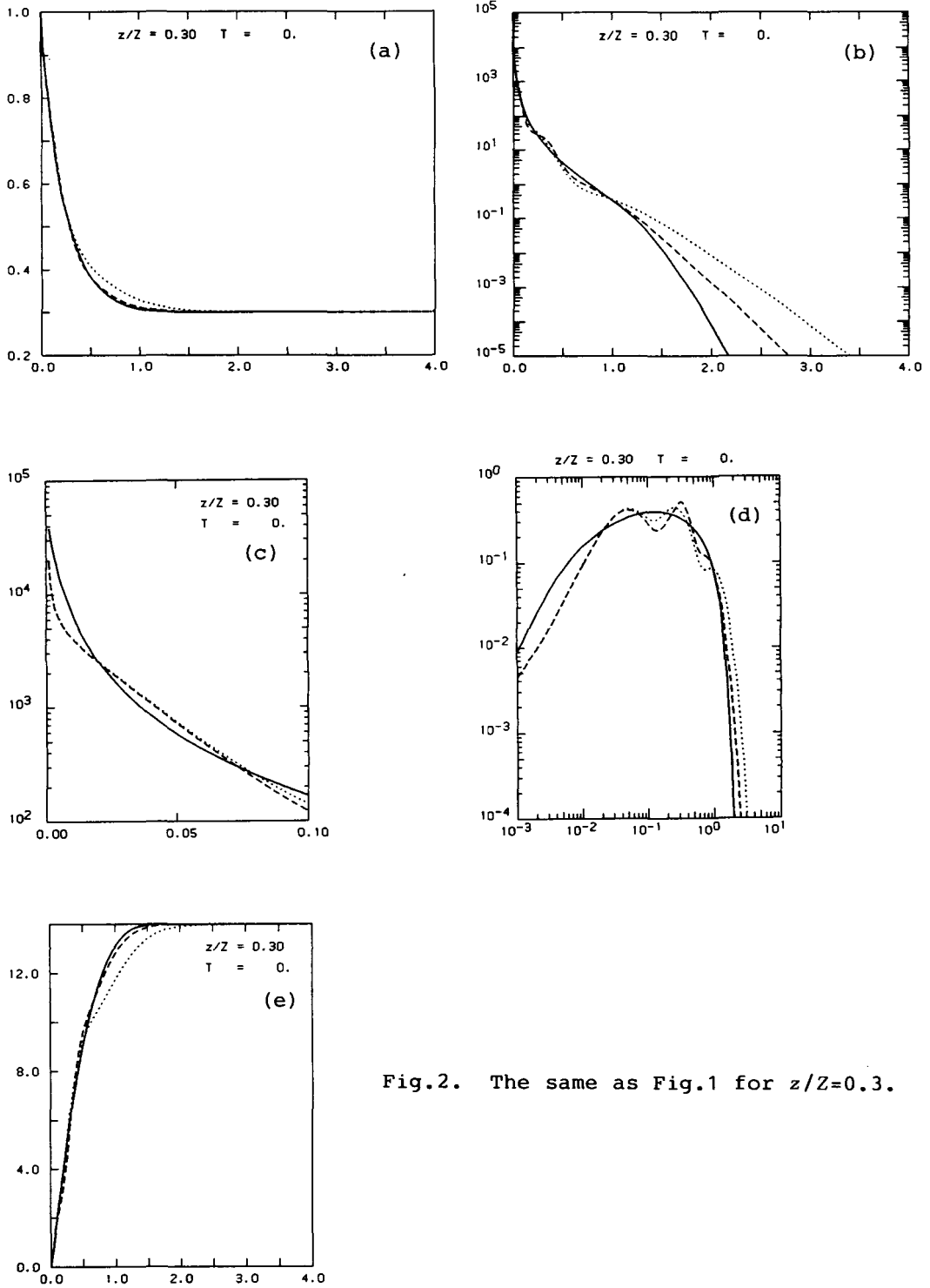


Fig.2. The same as Fig.1 for $z/Z=0.3$.

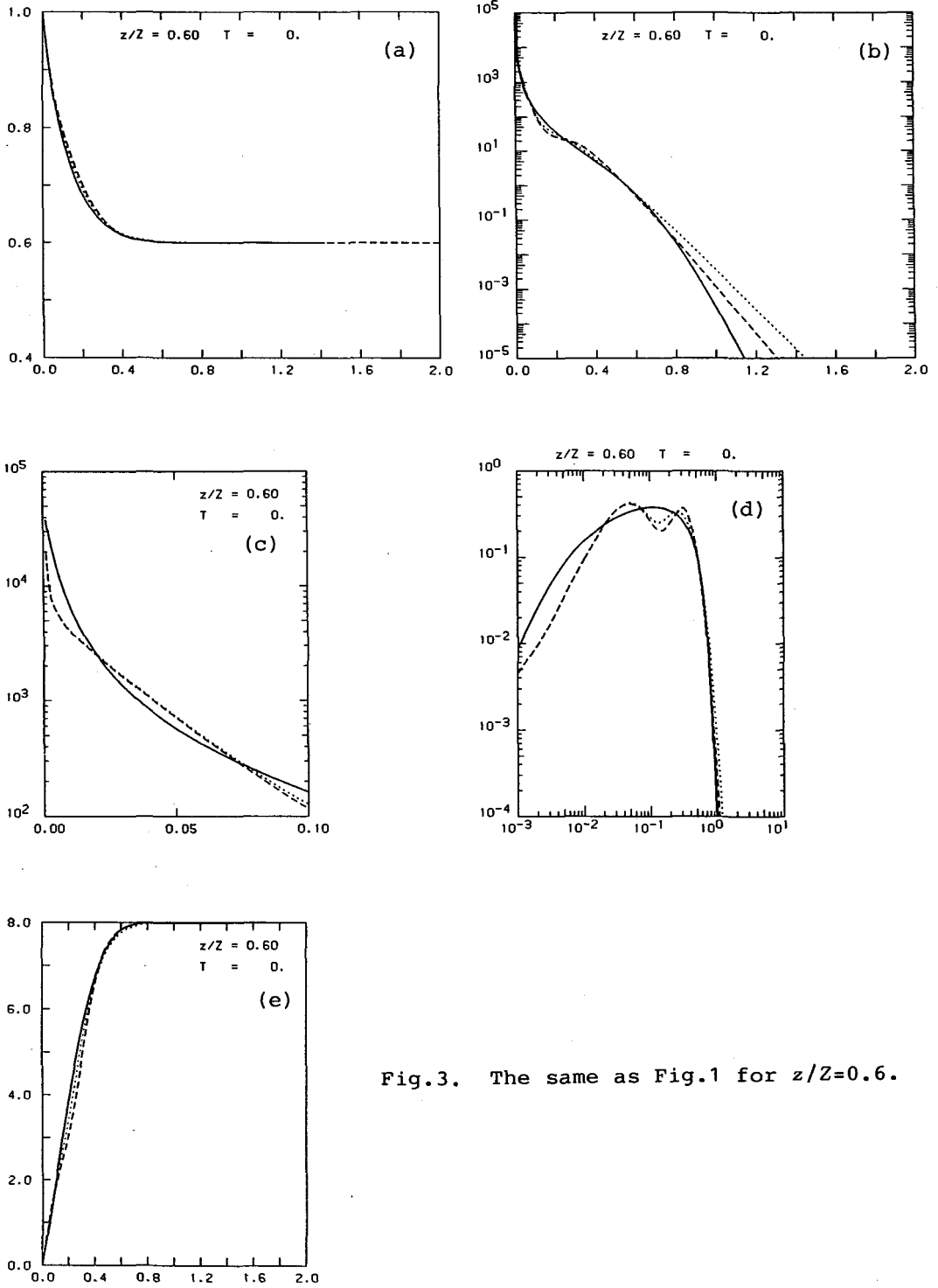


Fig.3. The same as Fig.1 for $z/Z=0.6$.

§4. Asymptotic Behavior of $n(r)$ and $\phi(r)$ as Solutions of the TFD and TFDW Equations

As was already pointed in I, our isolated ion model was constructed so as to satisfy the boundary conditions, $n'(R)=0$ and $U(r)=z/r$ for $r>R$, and the resultant electron density is discontinuous at $r=R$. In order to clarify in what sense our model ions are isolated, we now ask if there be a solution such that $n(R)=n'(R)=0$ at some finite (or infinite) radius. We are then led to analyze the asymptotic solutions of the TFD and TFDW equations.

A. $T=0$ case

In this case, the TFD equation gives a solution for $n(r)$ at a finite radius R where the decreasing function $\phi(r)$ vanishes. Since we know that

$$\frac{Z}{r}\phi(r) = K_T \left(n^{1/3} + \frac{K_X}{4K_T} \right)^2, \quad (14)$$

this requires $\phi(r) \geq 0$ and thus we cannot continue to evaluate $n(r)$ beyond R . As a result, $n(r)$ has a discontinuity at R , such that

$$n(R-0) = \left(-\frac{K_X}{2K_T} \right)^3 > 0 \quad \text{and} \quad n(r)=0, \quad r > R \quad (15)$$

and the chemical potential μ is related to R as

$$\mu = -U(R) - \frac{K_X^2}{4K_T} = -\frac{z}{R} - \frac{1}{2\pi^2}. \quad (16)$$

In the TFDW model, however, the above discontinuity of $n(r)$ is smeared out by the effect of squared gradient terms and no simple relation such as eq.(14) is available for $\phi(r)$. Assuming the asymptotic behavior as

$$U(r) \approx \frac{z}{r}, \quad \phi(r) \approx \frac{\mu}{Z} r + \frac{z}{Z} + \phi^{(1)}(r) \quad \text{and} \quad n(r) \rightarrow 0, \quad (17)$$

eq.(3.3) of I suggests

$$\phi^{(4)}(r) \approx \frac{1}{2} \frac{[\phi^{(3)}]^2}{\phi^{(2)}} - 36 \mu \phi^{(2)}, \quad (18)$$

which, upon integration, yields

$$\phi^{(1)}(r) \approx C \exp(-(-72\mu)^{1/2} r) \quad (19)$$

and the ionic radius becomes infinite as in the case of the TF model for a neutral atom. The chemical potential μ is determined by an asymptotic value of $\phi(r)$.

The above two solutions are likely to support our isolated ion model. We compare them with those of numerical analysis, for several values of z/Z , in Figs.4 to 6 and Table 2. We observe that $n(r)$ has essentially the same profile except for very small and large values of R and the effect of the gradient correction on μ is minute and less than a few per cent. In this sense, we may safely adopt the simple TFD model instead of the TFDW model, whenever we are concerned with quantities as evaluated by an integral over all electrons.

Table 2. Comparison between chemical potentials in TFDW and TFD models

| z/Z | 0.1 | 0.3 | 0.6 |
|-------|--------|--------|---------|
| TFDW | -0.894 | -4.452 | -17.913 |
| TFD | -0.844 | -4.348 | -17.727 |

B. $T > 0$ case

With the help of the finite temperature expressions for F_K and F_X , the TFD equation is written as

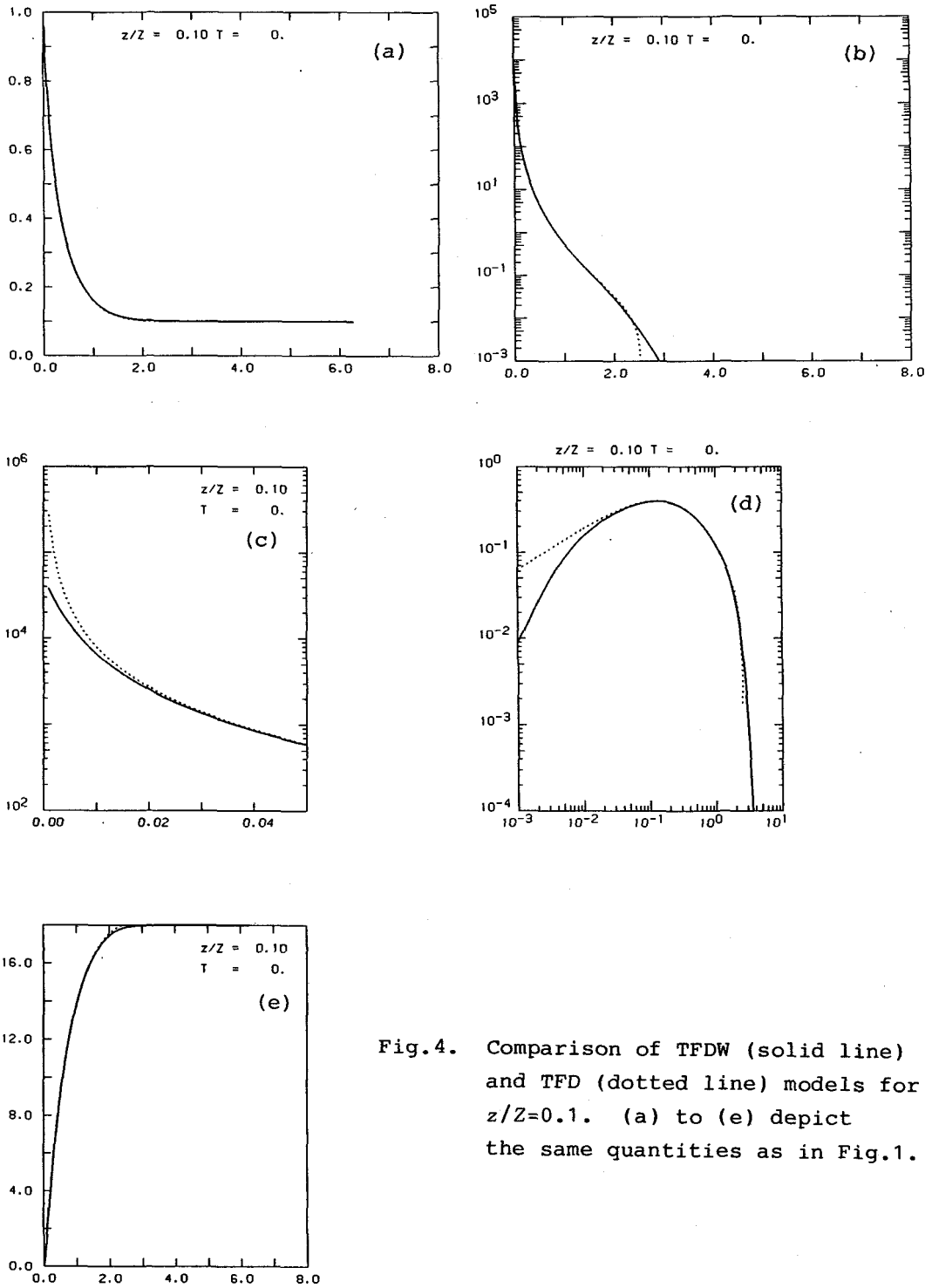


Fig.4. Comparison of TFDW (solid line) and TFD (dotted line) models for $z/Z=0.1$. (a) to (e) depict the same quantities as in Fig.1.

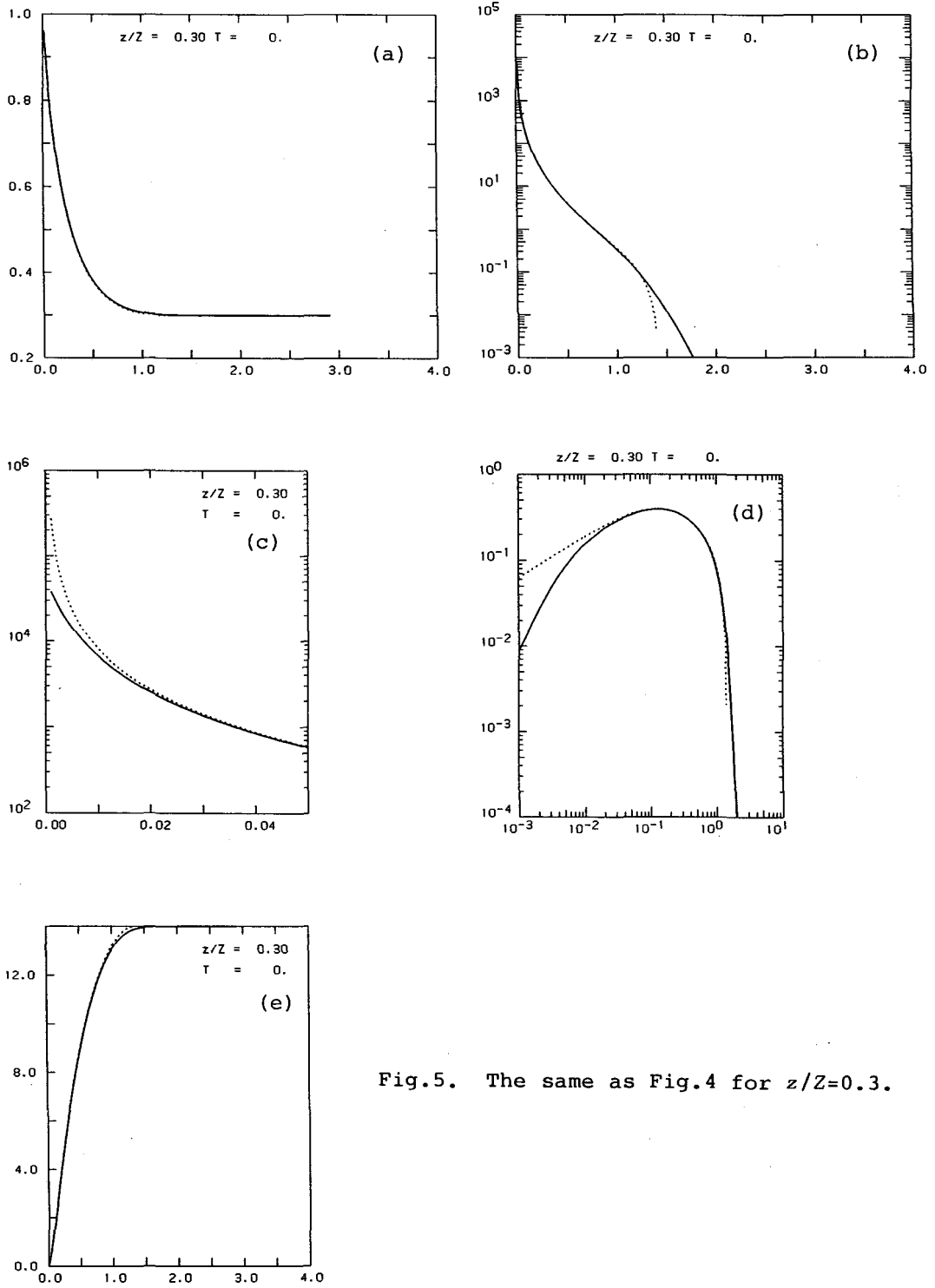


Fig.5. The same as Fig.4 for $z/Z=0.3$.

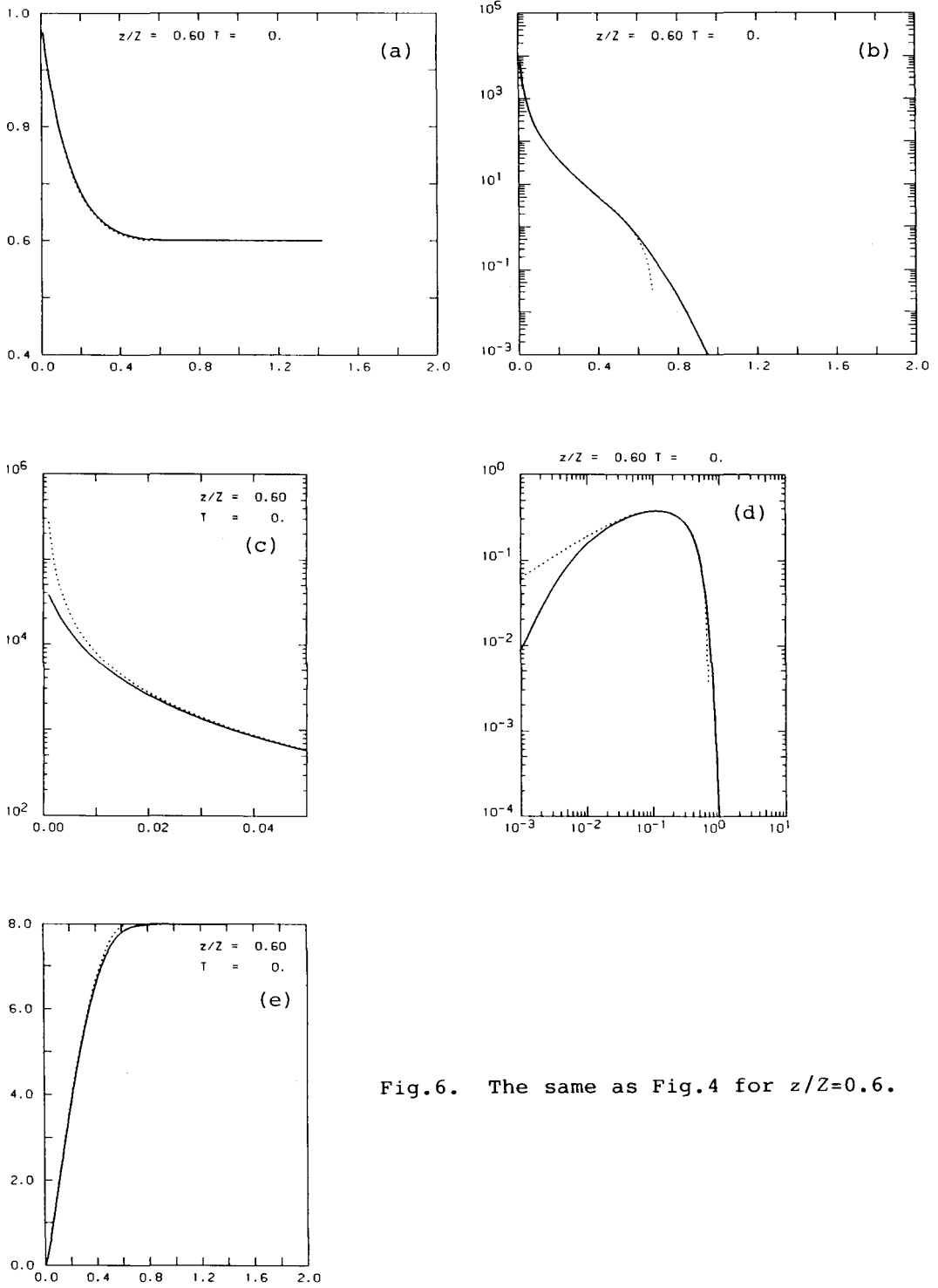


Fig.6. The same as Fig.4 for $z/Z=0.6$.

$$\frac{\partial F_K}{\partial n} + \frac{\partial F_X}{\partial n} - \frac{Z}{r} \phi + \frac{1}{2\pi^2} = 0, \quad (7)$$

which does not serve to limit the range of variation of ϕ , in marked contrast to the $T=0$ case. We may therefore expect to obtain $n(r)$, for example, which decreases continuously at large distances. Since the parameter y defined by eq.(4) decreases with $n(r)$, the kinetic and exchange energy densities can be approximated by

$$\frac{\partial F_K}{\partial n} = \frac{\alpha}{\beta} \quad \text{and} \quad \frac{\partial F_X}{\partial n} \approx e^\alpha \quad (20)$$

with $\alpha = \ln(2y/\pi^{1/2})$. Eq.(7) reduces then to

$$\frac{\partial F_K}{\partial n} \approx \frac{Z}{r} \phi - \frac{1}{2\pi^2}, \quad (21)$$

the solution of which can be given by

$$n(r) \approx \frac{1}{2^{1/2}(\pi\beta)^{3/2}} \exp\left\{\beta\left(\frac{Z}{r} \phi - \frac{1}{2\pi^2}\right)\right\} \approx \frac{1}{2^{1/2}(\pi\beta)^{3/2}} \exp(\beta\mu). \quad (22)$$

The above behavior of $n(r)$ at large distances is inconsistent with our original assumption. We may then conclude that the TFD equation for finite temperatures has no solution which describes the completely isolated ion.

In the case of the TFDW model, the asymptotic solutions satisfy

$$\phi^{(4)}(r) \approx 12 \phi^{(2)} \left[\frac{\alpha}{\beta} + \frac{1}{24} \left(\frac{\phi^{(3)}}{\phi^{(2)}} \right)^2 \right]. \quad (23)$$

This equation seems also to allow no decaying solution for $n(r)$ at large distances. It is obvious that the density decreasing with r by inverse power law is not acceptable, and its possible form may be Gaussian, such as $n(r) \propto \exp(-Ar^2)$ with $A = -6/\beta$, which is again inconsistent with the initial assumption. As shown above, the failure of describing an isolated ion by finite temperature TFD or TFDW models

may be ascribed to the use of the finite temperature version of F_k for small $n(r)$ on the outskirts of the ion, where applicability of these statistical models turns out questionable. Analysis from this point of view will be given elsewhere.

For practical purposes, however, we may adopt a solution for $n(r)$ of these equations, if it takes on a minimum value much smaller than a typical value within the ion, before it diverges. In effect, we find solutions of this type for the TFDW model in the case of large degree of ionization. Several examples are shown in Figs.7 to 9.

§5. Concluding Remarks

We have revised our previous solution for the one-electron Schrödinger equation,⁷⁾ taking the exchange-correlation potential into account. Except for the case of very small degree of ionization, we have thus obtained a sufficient number of bound states to confine electrons as required by the degree of ionization and these levels can be use as an initial input to the DFT formalism. The self-consistent solution of the latter has been obtained by an iterative procedure. Resultant electron distributions in the DFT are in satisfactory agreement with those obtained from the TFDW model.

In view of looking for a solution for $n(r)$ which satisfies the boundary conditions $n'(R)=n(R)=0$ simultaneously, we examined its asymptotic behavior using both the TFD and TFDW equations. For $T=0$, the TFDW equation provides us with such a solution which is essentially the same as the TFD solution with discontinuity, as far as quantities smeared over all electrons in the ion core are concerned, justifying thus the use of the simple TFD instead TFDW equations. When $T>0$, the TFDW equation has a solution for $n(r)$ with a minimum which can be regarded as zero for practical purposes, while the TFD equation seems to have no physically relevant solutions.

Our numerical code developed for the isolated ion model may easily be extended to a more realistic model with larger radius of several times the mean ionic distance, in which one includes neighboring ions and free electrons. This model allows us to take account of a screening effect of the surrounding particles and the correlations between different species of charged particles. Numerical analysis of such a model will be undertaken in the near

future.

Acknowledgements

We acknowledge Drs. K. Mima and H. Takabe for enlightening discussions and valuable comments. Numerical computations have been done at the Okayama University Computer Center. This work is supported in part by the Grant-in-Aid for Scientific Research of the Ministry of the Education, Science and Culture.

References

- 1) Y. Furutani, M. Shigesada and H. Totsuji, J. Phys. Soc. Japan 55, 2653(1986).
- 2) F. Perrot, Phys. Rev. A20, 586(1979).
- 3) S. Tanaka, S. Mitake and S. Ichimaru, Phys. Rev. A32, 1896(1985).
- 4) K. S. Singwi, M. P. Tosi, R. H. Land, and A. Sjölander, Phys. Rev. 176, 589(1968).
- 5) For example, F. Perrot, Phys. Rev. A25, 489(1982).
- 6) For example, M. W. C. Dharma-wardana and F. Perrot, Phys. Rev. A26, 2096(1982).
- 7) H. Takabe, K. Mima, H. Totsuji and Y. Furutani, presented at the annual meeting of Physical Society of Japan, March 1987, 28aJC2.

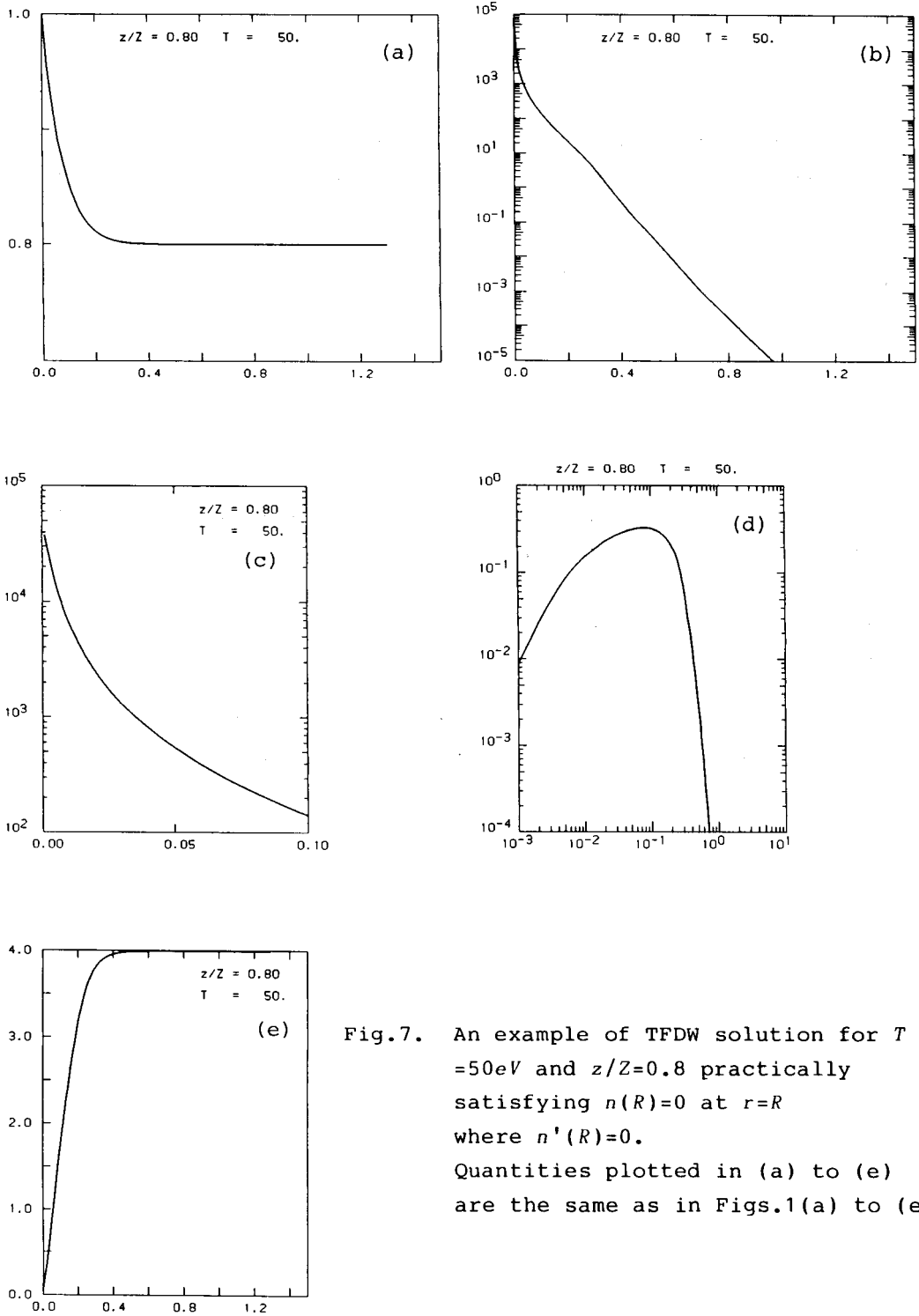


Fig.7. An example of TFDW solution for $T = 50eV$ and $z/Z=0.8$ practically satisfying $n(R)=0$ at $r=R$ where $n'(R)=0$. Quantities plotted in (a) to (e) are the same as in Figs.1(a) to (e)

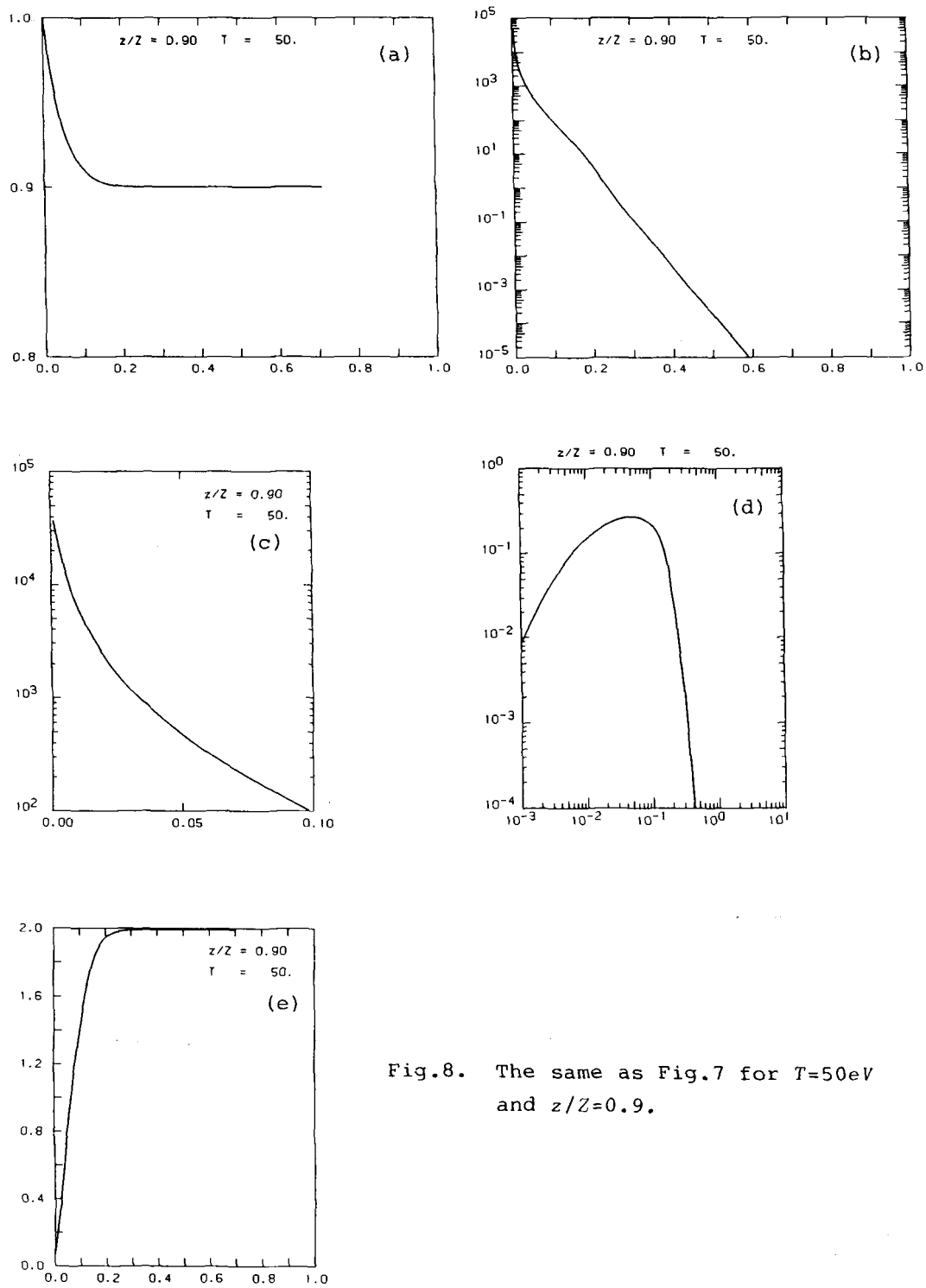


Fig.8. The same as Fig.7 for $T=50\text{eV}$ and $z/Z=0.9.$

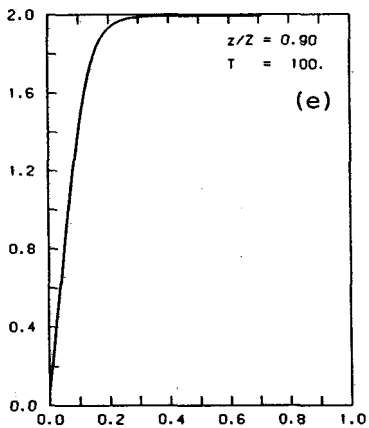
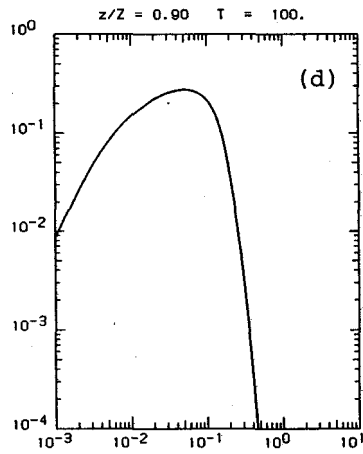
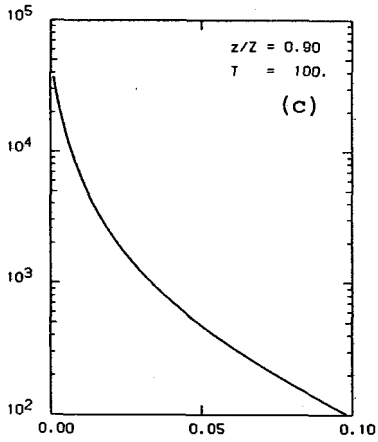
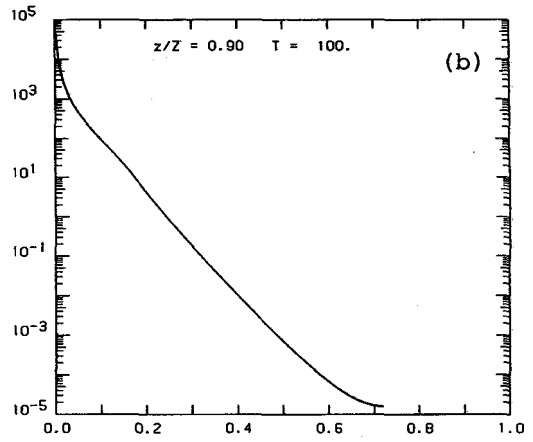
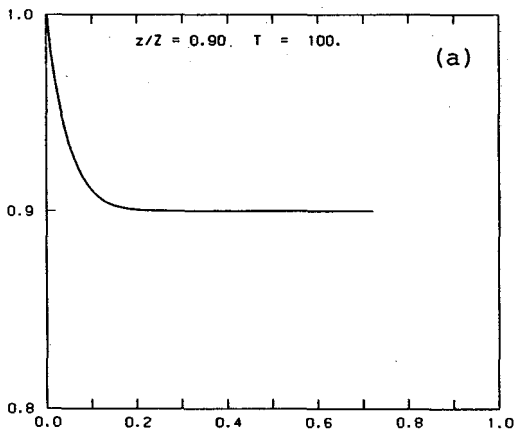


Fig.9. The same as Fig.7 for $T=100\text{eV}$ and $z/Z=0.9$.